

Thermodynamic Construction of an One-Step Replica-Symmetry-Breaking Solution in Finite Connectivity Spin Glasses

T. Nakajima^{1,*} and K. Hukushima^{1,†}

¹*Department of Basic Science, the University of Tokyo,
3-8-1 Komaba, Meguro-ku, Tokyo 153-8902 Japan*

(Dated: September 14, 2021)

An one-step replica-symmetry-breaking solution for finite connectivity spin-glass models with K body interaction is constructed at finite temperature using the replica method and thermodynamic constraints. In the absence of external fields, this construction provides a general extension of replica symmetric solution at finite replica number to one-step replica-symmetry-breaking solution. It is found that this result is formally equivalent to that of the one-step replica-symmetry-breaking cavity method. To confirm the validity of the obtained solution, Monte Carlo simulations are performed for $K = 2$ and 3. The thermodynamic quantities of the Monte Carlo results extrapolated to a large-size limit are consistent with those estimated by our solution for $K = 2$ at all simulated temperatures and for $K = 3$ except near the transition temperature.

PACS numbers: 64.60.De, 75.50.Lk

I. INTRODUCTION

Since the celebrated paper by Edwards and Anderson[1], mean-field theory of spin glass (SG) has been extensively investigated. The replica theory[2, 3] is one of the most successful achievement that has revealed the nature of the low temperature phase of mean-field SG models. Parisi's pioneering work provided the replica method with implementation of replica symmetry breaking (RSB). Originally, K step RSB (K RSB) was proposed as "a sequence of approximated solutions" to the true solution and the full RSB solution was derived as a $K \rightarrow \infty$ limit. This approach has actually proven to be exact recently[4] for the Sherrington-Kirkpatrick (SK) model[5]. Although this introduction of RSB is motivated by de Almeida-Thouless (AT) condition[6], which is the instability of replica symmetric (RS) solution with respect to replica couplings, it should be noted that AT instability is only one of the possible scenario for RSB[7] and that the origin of RSB is in general model-dependent. In addition, a 1RSB solution for various mean-field SG models[8, 9] is stable with respect to further RSB perturbation, and K RSB rarely appears for $K \geq 2$. These facts suggest that there is another mechanism to break the replica symmetry and it distinguishes 1RSB from full RSB (FRSB).

Recently, the authors have shown[10] that p -body SK model, which is a typical model to exhibit a SG transition to 1RSB phase, actually has another reason to break the replica symmetry above the Gardner temperature[8]. It is the monotonicity condition of the cumulant generating function of the free energy $\phi(n)$, whose limiting value at $n = 0$ is the averaged free energy, rather than the AT condition that causes RSB[10]. The relevance

of these conditions is reversed at the Gardner temperature, where the transition between 1RSB and full RSB takes place. Furthermore, it is proved that if the monotonicity is broken in the absence of external field, which ensures the smallest overlap parameter $q_0 = 0$, then the correct 1RSB solution is given by the RS solution at n_m , which is defined as the monotonicity breaking point, *i.e.*, $\phi'(n_m) = 0$. This has revealed that the continuation of the cumulant generating function $\phi(n)$ to $\phi(0)$ is strongly restricted by a kind of thermodynamic constraints and that it naturally induces the 1RSB solution in the case of a fully connected mean-field SG model. Regarding n as a fictitious inverse temperature, we can resort to the thermodynamics for extracting high-temperature, or replica, limit ($n \rightarrow 0$) from low-temperature behavior ($n \gg 1$). These facts strongly suggest that 1RSB is a consequence of the monotonicity breaking and FRSB is that of AT stability breaking.

Finite connectivity SG model has been considered as a first non-trivial extension of the mean-field theory, and challenged in many literatures. As a straight-forward extension from the case of fully connected model, perturbation theories in the region of the large connectivity or near the transition temperature have been studied in the replica formalism[11, 12]. Another replica calculation[13, 14, 15] has succeeded to derive an exact expression of the free energy under a non-trivial ansatz called factorized ansatz. The difficulty in these works appears in the search for an RSB saddle-point, because RSB is defined using the symmetry of a saddle-point in the theory. In contrast, the cavity method turned out to be an alternative and promising approach to study the finite connectivity models within 1RSB scheme[13, 16, 17, 18, 19]. The key concept of this method is the complexity[20], logarithm of a number of the pure states, which enables one to deeply understand the microscopic structure of configuration space. It is found that the non-negativity condition of the complexity is relevant for the 1RSB cavity scheme, that provides

*Electronic address: tetsuya@huku.c.u-tokyo.ac.jp

†Electronic address: hukusima@phys.c.u-tokyo.ac.jp

a general procedure for mean-field type models including finite connectivity SG.

In this paper, we further examine the possibility of 1RSB scenario suggested in our previous work, which might be important for a better understanding of the SG theory and also the replica method itself. The model discussed is a finite-connectivity Ising SG model with K -body interactions. The reason why this model is considered as a good example is twofold. First our construction of 1RSB solution is applicable to the finite-connectivity SG model, because RS solution can be explicitly obtained. Second, we see a direct correspondence between the guiding principle of introducing 1RSB in the replica method and the cavity method[13].

The organization of this paper is as follows. In Sec. II, we review our previous work[10] for complete and detailed instructions of our scheme, in which a construction of a 1RSB solution from RS ansatz is explained. Then a SG model defined on a sparse random graph is introduced and the 1RSB solution for the model obtained by our scheme is presented. We also discuss a relationship between our scheme based on the replica theory and the cavity method for the model. In Sec. III, we compare the 1RSB solution to the result by MC simulation. Finally Sec. IV is devoted to our conclusions and discussions.

II. MODEL AND REPLICA ANALYSIS

A. Preliminary

In this section, we briefly review our previous work[10] and explain our scheme for the construction of a 1RSB solution in a general manner. For a given Hamiltonian H , equilibrium statistical mechanics requires to calculate the partition function $Z = \text{Tr} \exp(-\beta H)$, where Tr denotes the sum over all possible configurations of the dynamical variables and $\beta = 1/T$ is the inverse temperature. In the case of disordered system, one may evaluate $Z(\mathbf{J})$ for quenched disorder \mathbf{J} and take average of $\log Z(\mathbf{J})$ over \mathbf{J} with an appropriate weight. Using the replica method[3], the averaged free energy $[F]$ is rewritten as a limit of cumulant generating function $\phi(n)$ of $F(\mathbf{J})$ as

$$[F] = \lim_{n \rightarrow 0} \left\{ -\frac{1}{N\beta n} \log[Z^n] \right\} =: \lim_{n \rightarrow 0} \phi(n), \quad (1)$$

where $[\dots]$ denotes the average with respect to the quenched disorder.

In case where n is a real number, to proceed the calculation of the right hand side in Eq. (1) needs some ansatz. A typical one is replica symmetric (RS) ansatz, which is considered to be correct only for sufficiently large n . We denote the solution based on the RS ansatz as RS solution $\phi_{\text{RS}}(n)$. Thus, the limit of $\phi(n)$ we are interested in becomes nontrivial when we have no alternatives except the RS solution.

In general, however, the function $\phi(n)$ is restricted by the following conditions: $\phi'(n) \leq 0$ (monotonicity),

$(n\phi(n))'' \leq 0$ (convexity), and AT stability. The two former conditions, monotonicity and convexity, come from a thermodynamic restriction if the replica number n is regarded as a ‘‘temperature’’. In particular, they lead to the following proposition[10]:

$$\begin{aligned} & \text{if } \phi'(n_m) = 0 \text{ for } n_m > 0, \\ & \text{then } \phi(n) = \phi(0) \text{ for } 0 \leq n \leq n_m. \end{aligned}$$

Therefore, if the RS solution is valid for $n \geq n_m$, the limit $n \rightarrow 0$ is performed by this proposition. Figure 1 shows how the function ϕ is connected to the origin. It is also shown[10] that the solution $\phi_{\text{RS}}(n_m)$ corresponds to the 1RSB solution for a wide class of models with $q_0 = 0$, not restricted to the fully connected models. This relationship has already been pointed out in a solvable model[21].

The proposition provides us a simple construction of a 1RSB solution using only the RS solution. We summarize our procedure for the 1RSB construction as follows:

1. Calculate the RS solution $\phi_{\text{RS}}(n)$ as a function of the finite replica number n .
2. Find the value n_m which satisfies $\phi'_{\text{RS}}(n_m) = 0$.
3. Set

$$\phi(0) = \phi_{\text{RS}}(n_m). \quad (2)$$

While the right hand side of Eq. (2) is analytically tractable but doubtful for $n \ll 1$ because of the RS ansatz, the left hand side is equal to the free energy as stated in Eq. (1) but analytically intractable.

One may notice that this procedure is analogous to the original saddle-point method, if one identifies the replica number with the breaking parameter. We consider this correspondence as the reason why we have to maximize with respect to the breaking parameter in literatures. It should be noted that this procedure can apply to any model in which the RS solution is explicitly obtained for any real n . Our procedure does not require overlap matrix or the introduction of breaking parameter.

B. Model

Hereafter we deal with a finite-connectivity Ising SG model. The Hamiltonian with K -spin interactions on a regular random graph with connectivity C is defined as:

$$H = - \sum_{\mu \in \mathcal{G}} \mathcal{D}_\mu J_\mu \sigma_{\mu(1)} \sigma_{\mu(2)} \cdots \sigma_{\mu(K)}, \quad (3)$$

where

$$\mathcal{G} = \left\{ \mu = \{\mu(1), \dots, \mu(K)\}; \right. \\ \left. \mu(i) \in \{1, 2, \dots, N\}, \mu(i) \neq \mu(j) (i \neq j) \right\}. \quad (4)$$

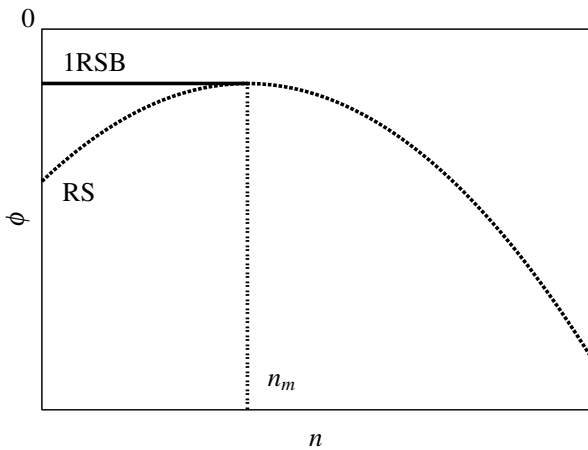


FIG. 1: A schematic figure of $\phi(n)$ as a function of the replica number n . This shows the construction of a 1RSB solution using monotonicity and convexity condition. The dashed line represents RS solution, which breaks the monotonicity condition at $n = n_m$. Below n_m , $\phi(n)$ becomes a constant function down to zero, corresponding to the 1RSB solution.

Here $\sigma_i = \pm 1$ represents Ising spins on the random graph with N sites. The interactions J_μ take ± 1 with equal probability which gives the unit of energy and temperature. $\mathcal{D}_\mu = 0, 1$ are quenched variables, satisfying the condition $\sum_{\mu \in \mathcal{G}, i \in \mu} \mathcal{D}_\mu = C$ for each site i , namely all the sites having the same number of the neighbors C .

C. Solutions for 1RSB

We calculate the cumulant generating function of the model described above within the framework of Sec. II A. Following the calculation[22, 23, 24], $\phi(n)$ under the RS ansatz is evaluated as

$$\phi_{\text{RS}}(n) = -\frac{C}{K\beta} \log(\cosh(\beta)) - \frac{1}{\beta n} \text{extr}_{\pi, \hat{\pi}} \left\{ \frac{C}{K} \log I_1 - C \log I_2 + \log I_3 \right\}, \quad (5)$$

where

$$I_1 = \int \prod_{k=1}^K dx_k \pi(x_k) \frac{1}{2} \sum_{J_\mu = \pm 1} \left\{ 1 + \tanh(\beta J_\mu) \prod_{k=1}^K \tanh(\beta x_k) \right\}^n, \quad (6)$$

$$I_2 = \int dx d\hat{x} \pi(x) \hat{\pi}(\hat{x}) \{1 + \tanh(\beta x) \tanh(\beta \hat{x})\}^n, \quad (7)$$

$$I_3 = \int \prod_{\gamma=1}^C d\hat{x}_\gamma \hat{\pi}(\hat{x}_\gamma) \left\{ \prod_{\gamma=1}^C (1 + \tanh(\beta \hat{x}_\gamma)) + \prod_{\gamma=1}^C (1 - \tanh(\beta \hat{x}_\gamma)) \right\}^n. \quad (8)$$

Differentiating ϕ_{RS} with respect to π and $\hat{\pi}$, we have the saddle-point equations

$$\pi(x) = \frac{I_2}{I_3} \int \prod_{\gamma=1}^{C-1} d\hat{x}_\gamma \hat{\pi}(\hat{x}_\gamma) \left\{ \prod_{\gamma=1}^{C-1} (1 + \tanh(\beta \hat{x}_\gamma)) + \prod_{\gamma=1}^{C-1} (1 - \tanh(\beta \hat{x}_\gamma)) \right\}^n \delta \left(x - \sum_{\gamma=1}^{C-1} \hat{x}_\gamma \right), \quad (9)$$

$$\hat{\pi}(\hat{x}) = \frac{I_2}{I_1} \int \prod_{k=1}^{K-1} dx_k \pi(x_k) \frac{1}{2} \sum_{J_\mu = \pm 1} \delta \left(\hat{x} - \frac{1}{\beta} \text{atanh} \left(\tanh(\beta J_\mu) \prod_{k=1}^{K-1} \tanh(\beta x_k) \right) \right). \quad (10)$$

We solve Eqs. (9) and (10) for each n numerically and obtain the saddle-point functions $\pi(x)$ and $\hat{\pi}(\hat{x})$. Details for the numerical method we use to solve these equations are shown in Appendix A. Inserting the saddle-point functions into Eq. (5), we evaluate $\phi_{\text{RS}}(n)$ as a function of n . Fig. 2 shows an example of $\phi_{\text{RS}}(n)$ plotted against n for $K = 3$ and $C = 4$ at $T = 0.33$, which is well below the expected SG transition temperature, $T_c \approx 0.65$. As

shown in the figure, $\phi_{\text{RS}}(n)$ violates the monotonicity condition at a certain value $n_m(T)$ which is defined by $\phi_{\text{RS}}(n_m) = 0$.

Following our scheme mentioned above, this is enough to construct a 1RSB solution. The 1RSB free energy per site f is given as $f = \phi_{\text{RS}}(n_m)$. It would be interesting to see the information of finite replica number is used to describe the 1RSB free energy. This is a consequence

of the thermodynamic construction, with which the RS solution is connected to the physical limit $n \rightarrow 0$.

We have evaluated $\phi_{\text{RS}}(n)$ at $0 \leq n \leq 1$ for $K = 2$ and $K = 3$, which yields temperature dependence of the 1RSB free energy shown later. For comparison, we also evaluate an RS free energy, which is defined as $\phi_{\text{RS}}(0)$. Temperature dependence of n_m for some values of C is plotted for $K = 2$ and 3 in Fig. 3. We also show the parameter m for $K = 2$ and $C = 4$ in Fig. 3, evaluated in Ref. 18. They are in good agreement with each other. The transition temperature for $K = 2$ is derived from the condition that the instability condition of $\pi(x) = \delta(x)$ and then n_m begin to deviate from zero. The estimate of T_c is consistent with the known expression $T_c = 1/\text{atanh}(C - 1)$ [25] considering an appropriate factor $\sqrt{1/C}$. For $K = 3$, T_c is determined by an onset temperature at which the monotonicity breaking point emerges. Then, n_m deviates from unity, that is often observed in some models exhibiting 1RSB transition. While the analytic expression of T_c for $K = 3$ has not known yet, the estimate for $C = 4$ and 8 is consistent with that obtained by the cavity method[16].

Here we compare our scheme to the established cavity method, in particular for the finite connectivity Ising SG model[16]. The saddle-point equations, Eqs. (9) and (10), in our scheme are the same as the recursion equation derived as Eqs. (A.3) and (A.4) in Ref. 16, when the functions π and $\hat{\pi}$ are identified as the distribution of cavity field and cavity bias, respectively. While the parameter n is determined by the monotonicity condition $\phi'(n) = 0$, the 1RSB parameter m in the cavity context is determined by the non-negativity condition of the complexity Σ :

$$\Sigma(f(m)) = \beta m^2 \phi'(m) = 0 \quad (11)$$

within the formalism of Monasson[20, 26]. This means that these two methods are equivalent when the complexity is a well-defined quantity.

In the previous works[13, 14, 16], it is shown that the result of the cavity method corresponds to that of the replica method with a factorized ansatz for the finite connectivity models. Thus, our construction is also equivalent to the replica theory with the factorized ansatz. In the formalism, the replica number n is substituted for the breaking parameter m in the expression of free energy without taking the limit $n \rightarrow 0$. Then, the maximization of the free energy with respect to the overlap parameter q and breaking parameter m is equivalent to the monotonicity breaking condition in our scheme. This reasoning does not give a correctness proof of the factorized ansatz (and also our) solution, but we convince ourselves that it reveals the reason why the factorized ansatz gives numerically correct solution.

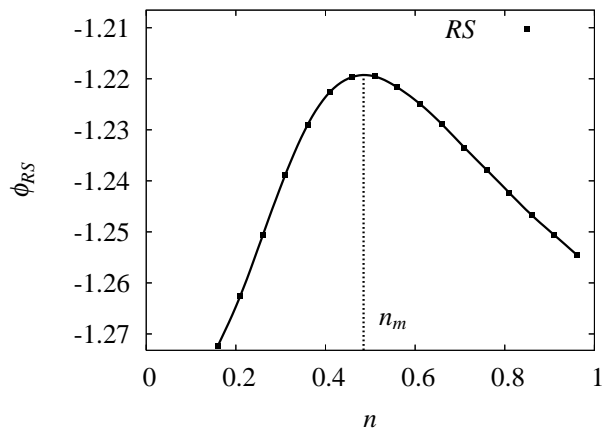


FIG. 2: Replica number n dependence of $\phi_{\text{RS}}(n)$ of a finite-connectivity Ising SG for $K = 3$ and $C = 4$ at $T = 0.33$.

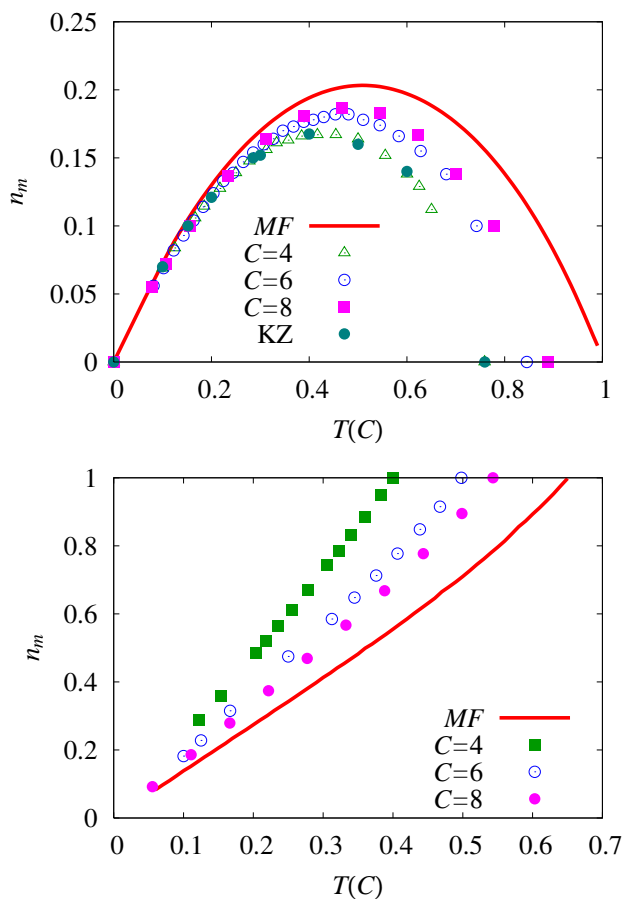


FIG. 3: (Color online) Temperature dependence of n_m for $K = 2$ (top panel) and for $K = 3$ (bottom panel). Temperature is scaled as $T(C) = T\sqrt{K/2C}$. Each mark represents n_m for connectivity $C = 4, 6$ and 8 . The solid line represents n_m for K -body Sherrington-Kirkpatrick model with Gaussian interaction. In the top panel, thermodynamic value of 1RSB parameter for $K = 2$ and $C = 4$ evaluated in Ref. 18 is also shown in filled circle.

III. VERIFICATION BY NUMERICAL SIMULATION

A. Monte Carlo method

In the previous section, we obtain the 1RSB solution for the Ising SG model with K -body interactions by using our scheme. This is the true solution if the AT instability or others would not occur above n_m , but it is difficult to examine the validity of $\phi_{RS}(n)$. This situation is similar to the case of the cavity method. Instead, here we verify our 1RSB solution by comparing it to Monte Carlo (MC) data. We use exchange MC method[27] in order to accelerate relaxation time to equilibrium. The number of temperatures is fixed to be 30 and the lowest temperature is down to 0.5 for all the system sizes N and K . The simulation parameters for $K = 2$ and $K = 3$ are presented in Table I and II, respectively. Equilibration of the MC simulations is confirmed by seeing that the observed quantities are stable within range of error by doubling MC steps.

By using the MC simulation we measure the energy $e_N(T)$ per site and calculate the free energy $f_N(T)$ per site by thermodynamic integration:

$$f_N(T) = T \int_T^\infty dT' \frac{e_N(T')}{T'^2}, \quad (12)$$

and the entropy $s_N(T)$ per site as

$$s_N(T) = \frac{e_N(T) - f_N(T)}{T}. \quad (13)$$

Through the data at discrete temperatures obtained by the exchange MC method, the energy as a continuous function of T is evaluated by reweighting formula[28]:

$$\langle A(\sigma) \rangle_{MC}^{(\beta)} = \frac{\langle A(\sigma) e^{(\beta_0 - \beta)H(\sigma)} \rangle_{MC}^{(\beta_0)}}{\langle e^{(\beta_0 - \beta)H(\sigma)} \rangle_{MC}^{(\beta_0)}}, \quad (14)$$

where $\langle \dots \rangle_{MC}^{(\beta)}$ denotes the MC average at the inverse temperature β . We apply this formula by setting β_0 as actually simulated temperature and β as required one. We choose β_0 as the nearest temperature to β from the whole set of simulated temperatures.

B. Results

We display thermodynamic quantities, energy, free energy and entropy, obtained by MC simulations, together with the RS and 1RSB solutions for $K = 2$ and $C = 4$ in Fig. 4 and for $K = 3$ and $C = 4$ in Fig. 5. The data show that in the case of $K = 2$, the RS and 1RSB solutions are close to each other, but the 1RSB free energy is always greater than the RS one by definition.

For $T > T_c$, the correct solution is given by the paramagnetic one, which is described by $\pi(x) = \hat{\pi}(x) = \delta(x)$.

N	N_{MCS}	N_s
32	1×10^5	4096
48	2×10^5	2048
64	4×10^5	1024
128	3×10^6	512
256	5×10^7	128
512	5×10^8	30

TABLE I: Parameters of simulation in the case of $K = 2$ and $C = 4$. The total number of Monte Carlo steps $2N_{\text{MCS}}$ and the total number of samples N_s are presented for each size N . The first N_{MCS} are discarded for equilibration and the subsequent N_{MCS} are used in measurement.

N	N_{MCS}	N_s
30	1×10^5	4096
36	1×10^5	4096
45	2×10^5	2048
60	4×10^5	1024
75	8×10^5	1024
120	3×10^6	512
240	1×10^8	128

TABLE II: Parameters of simulation in the case of $K = 3$ and $C = 4$. The total number of Monte Carlo steps $2N_{\text{MCS}}$ and the total number of samples N_s are presented for each size N . The first N_{MCS} are discarded for equilibration and the subsequent N_{MCS} are used in measurement.

For comparison, we also plot a practical solution based on frozen ansatz[29], in which the paramagnetic solution is used at $T > T_g$ and the entropy is kept to zero at $T < T_g$. Here T_g is defined as the temperature at which the entropy given by the paramagnetic solution is zero. This ansatz leads to the results that the free energy as well as the energy is independent of T below T_g . The frozen ansatz is interpreted as a paramagnetic solution on which the monotonicity condition as a function of temperature is imposed. Although the true free energy must be a monotonically decreasing function of temperature in a standard thermodynamic sense, it might not be a sufficient condition. In fact, MC data and the 1RSB solution are far from the frozen-ansatz solution. In particular, they show non-zero value of the entropy at finite temperatures as shown in the bottom of Fig. 4, which is quite different from that of the frozen ansatz.

For $K = 3$, we do not plot the RS solution because we cannot find it at low temperatures near $n = 0$ except for the paramagnetic one. This suggests that the 1RSB scheme works even if the RS solution does not exist near $n = 0$, though we cannot rule out the possibility that our algorithm for evaluating π is unstable to find the RS solution.

To see thermodynamic properties, we extrapolate our MC data with finite sizes to the thermodynamic limit $N \rightarrow \infty$. Because finite-size correction terms and its

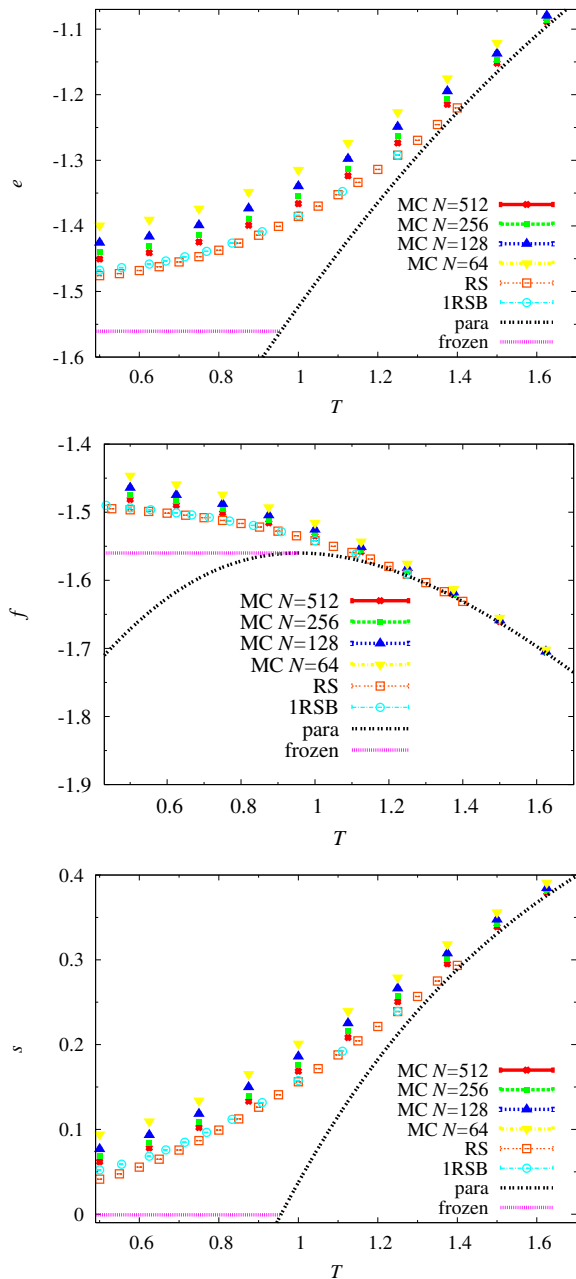


FIG. 4: (Color online) Temperature dependence of energy (top panel), free energy (middle panel) and entropy (bottom panel) for a finite connectivity Ising SG with $K = 2$ and $C = 4$. MC results are shown by filled marks for $N = 64, 128, 256$ and 512 from the top. Open squares and open circles are the results of the IRSB solution and the RS one, respectively. The paramagnetic solution is presented by the dotted line and the frozen ansatz is solid line.

exponent are a priori unknown in SG models, an extrapolation method itself should be investigated. We assume that the leading finite-size correction terms for the energy, free energy and entropy are expressed as

$$e_N = e_\infty + a_e \times N^{-\omega}, \quad (15)$$

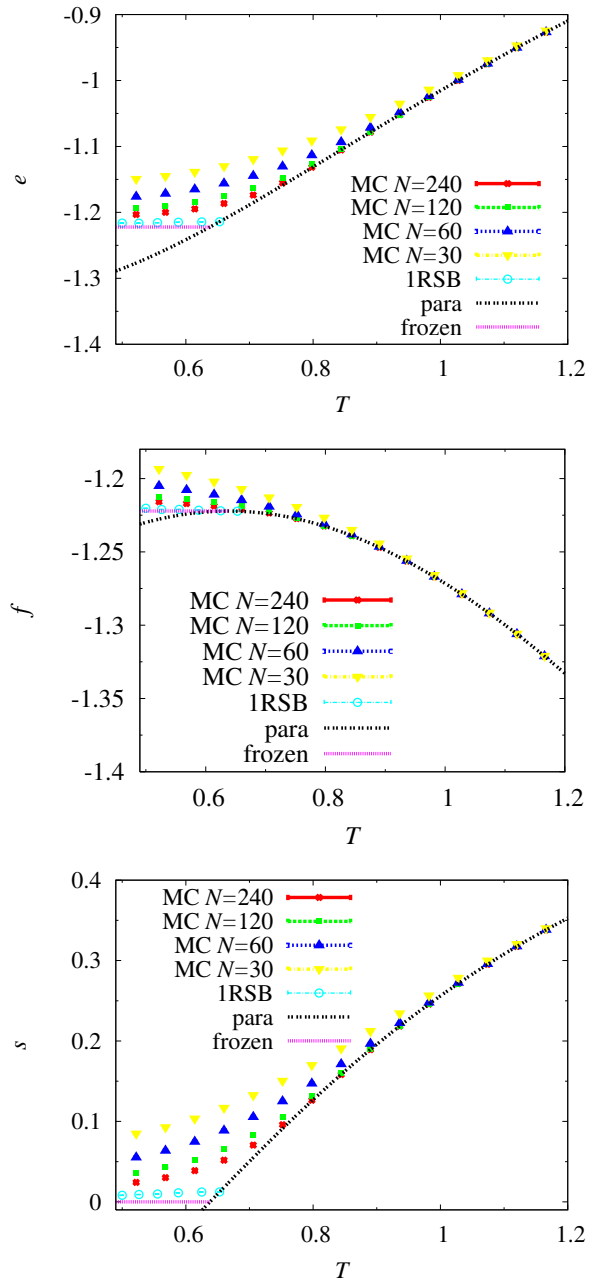


FIG. 5: (Color online) Temperature dependence of energy (top panel), free energy (middle panel) and entropy (bottom panel) for a finite-connectivity Ising SG with $K = 3$ and $C = 4$. MC results are shown by filled marks for $N = 30, 60, 120$ and 240 from the top. Details of the lines are the same as those of Fig. 4.

$$f_N = f_\infty + a_f \times N^{-\omega}, \quad (16)$$

$$s_N = s_\infty + a_s \times N^{-\omega}, \quad (17)$$

where e_∞ , f_∞ and s_∞ are the thermodynamic limit of the respective quantities, and the correction exponent ω is assumed to be independent of the quantities.

As shown in the previous work[30], the ground-state energy of the Ising SG model for $K = 2$ defined on a

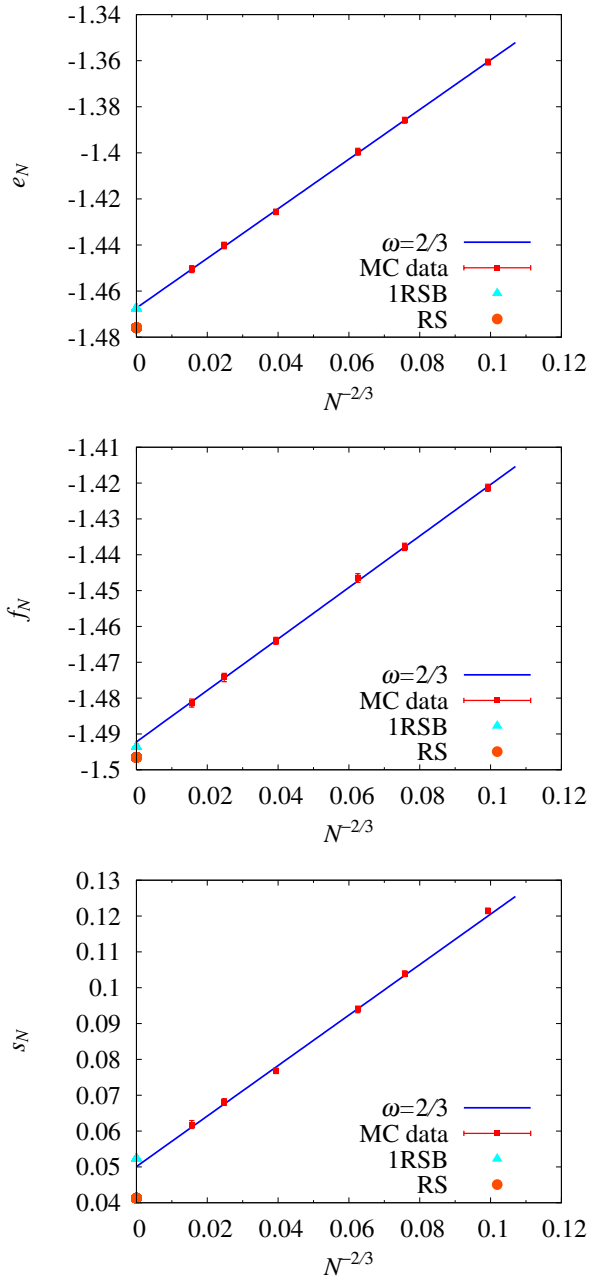


FIG. 6: (Color online) Energy, free energy and entropy as a function of $1/N^{2/3}$ for a finite-connectivity Ising SG with $K = 2$ and $C = 4$ at $T = 0.5$. The filled squares are MC results, filled triangle is 1RSB solution, and filled circle is RS solution. In solid line, the least square fitting of MC results assuming the exponent of the leading finite-size correction ω is $2/3$ is presented.

regular random graph is scaled with $\omega = 2/3$. Thus, we assume that the exponent $2/3$ holds for $K = 2$ at finite temperatures and is independent of physical quantities. Figs. 6 show the thermodynamic quantities as a function of $N^{-2/3}$ for $K = 2$ at $T = 0.5$, which is the lowest observed temperature. The data are fitted well with the

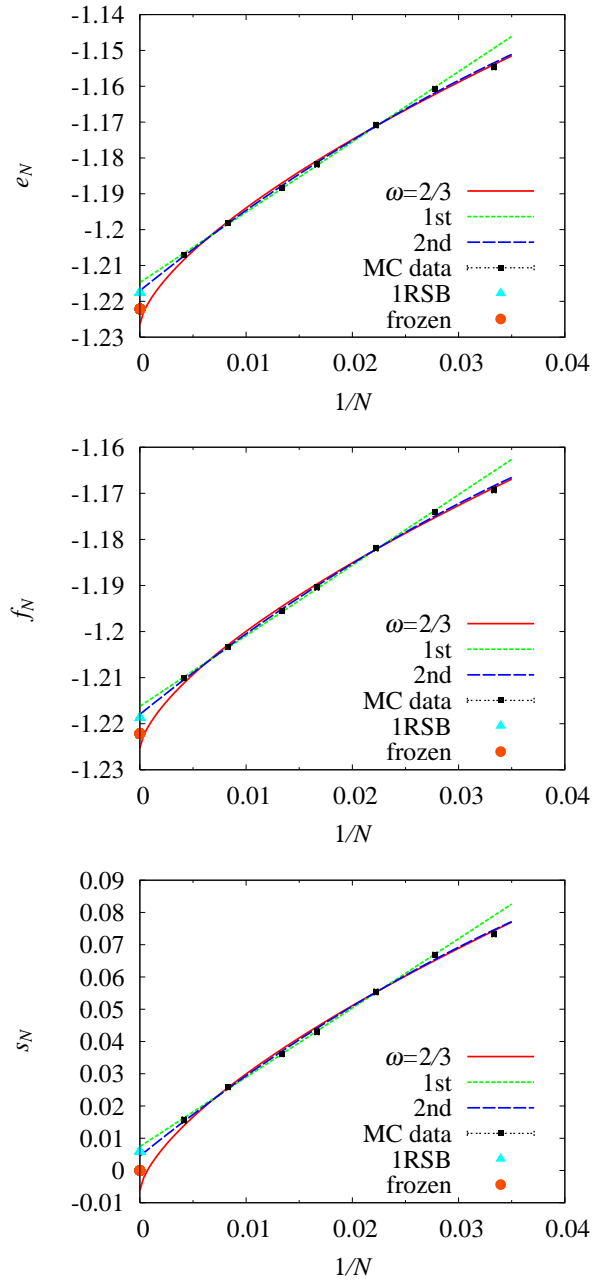


FIG. 7: (Color online) Energy, free energy and entropy as a function of $1/N$ for a finite-connectivity Ising SG with $K = 3$ and $C = 4$ at $T = 0.2$. The points and solid line are the same as in Figs. 6. Short-dashed and long-dashed lines represent the least-squares fits for the form including the leading term of $1/N$ and up to the next leading terms, respectively.

assumption $\omega = 2/3$ as shown in the figure. The extrapolated values by the best fit and the results by the 1RSB and the RS solutions are shown in Table III. The thermodynamic values by MC results agree with those by the 1RSB solution rather than the RS one. The energy extrapolated in a wide range of temperature is displayed in Fig. 8. This also suggests that the 1RSB solution is

	MC	1RSB	RS
e_∞	-1.4673(4)	-1.4675(2)	-1.4758(2)
f_∞	-1.4922(4)	-1.4937(1)	-1.4965(1)
s_∞	0.0501(9)	0.0522(2)	0.04128(2)

TABLE III: Thermodynamic limit of the energy, free energy and entropy of a finite-connectivity Ising SG for $K = 2$ and $C = 4$ at $T = 0.5$. 1RSB and RS represent those estimated from the 1RSB solution and the RS one, respectively. MC means the extrapolated values from finite-size MC data by assuming a power law of the leading correction with the exponent $\omega = 2/3$.

	MC	1RSB	frozen ansatz
e_∞	-1.217(1)	-1.2176(1)	-1.2221
f_∞	-1.2180(8)	-1.2188(1)	-1.2221
s_∞	0.005(2)	0.0058(5)	0

TABLE IV: Thermodynamic limit of the energy, free energy and entropy of a finite-connectivity Ising SG for $K = 3$ and $C = 4$ at $T = 0.2$. 1RSB and frozen ansatz represent those estimated from the 1RSB solution and the frozen-ansatz one. MC means the extrapolated values from finite-size MC data by assuming a form of $x_N = x_\infty + a_1 N^{-1} + a_2 N^{-2}$, where $x = e, f$ or s .

consistent with numerical results.

We turn to the case of $K = 3$, where the value of ω is not known even at zero temperature. Although a naive way to suppress higher order corrections is to study the system for large sizes and/or at lower temperatures apart from critical temperature, it has not been feasible to perform the MC simulation below $T = 0.5 \sim 0.7T_c$ for $N \geq 240$ in moderate CPU time because of extremely

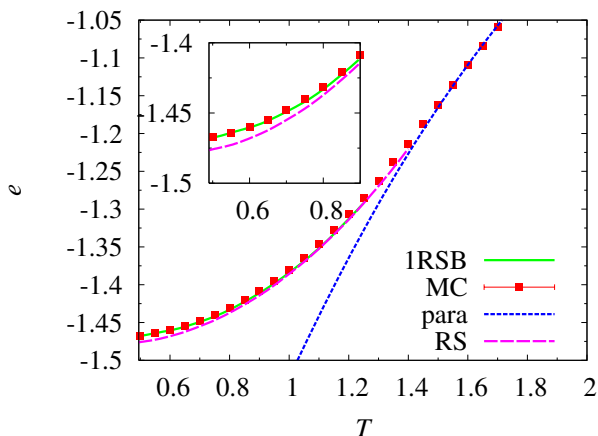


FIG. 8: (Color online) Temperature dependence of the energy for a finite-connectivity Ising SG for $K = 2$ and $C = 4$. The extrapolated value from MC data is marked by filled square. The 1RSB, RS and paramagnetic solutions are represented by solid, long-dashed and short-dashed lines, respectively. The inset is an enlarged view at low temperatures.

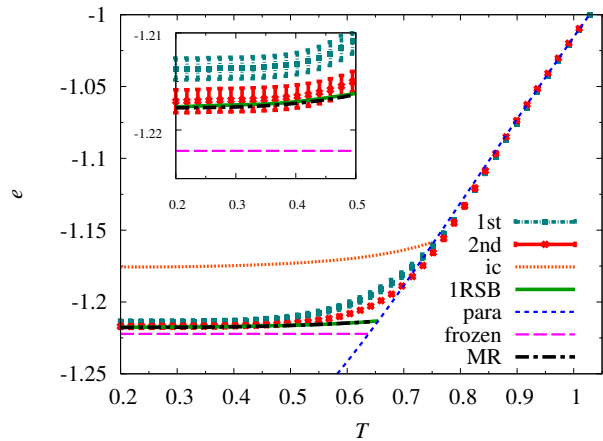


FIG. 9: (Color online) Temperature dependence of the energy for a finite-connectivity Ising SG for $K = 3$ and $C = 4$. The filled squares and cross marks are the extrapolated value from MC data with the extrapolation form including the leading correction term and up to the next correction terms, respectively. The 1RSB, frozen and paramagnetic solutions are represented by solid, long-dashed and short-dashed lines, respectively. Long-short-dashed line is the result of the cavity method in Ref. 16. The iso-complexity energy obtained in Ref. 16 is also shown by dotted line. The inset is an enlarged view at low temperatures.

slow relaxation especially in the case of $K = 3$. This is contrast to $K = 2$ model. However, for relatively smaller systems, the distribution function of the energy is found to be almost a delta function with the weight at the lowest energy. This implies that the distribution depends weakly only on temperature T below 0.5. This fact enables us to obtain the energy at temperatures down to $T = 0.2 \sim 0.3T_c$ using the reweighting method[28]. We evaluate the correction exponent ω for the energy by the least-squares estimation at $T = 0.2$ and 0.5 with a form of Eq. (15). The estimate of ω is not compatible with $\omega = 2/3$ used in the case of $K = 2$, and is rather close to $\omega = 1$. This tendency is enhanced by omitting the smallest size $N = 30$ from the analysis. These findings suggest that $\omega \simeq 1$ and higher order corrections are not negligible.

Therefore, we extrapolate the MC result for $K = 3$ by assuming the forms of Eqs. (15), (16) and (17) for $\omega = 1$ with the next leading correction term $1/N^2$. The data for $N = 30$ are omitted from the extrapolation analysis. Figures 7 shows the result of the thermodynamic quantities for $K = 3$ and $C = 4$ at $T = 0.2$. The extrapolated values, presented in Table IV, are consistent with those of the 1RSB solution by taking into account the next leading correction term.

We also show the thermodynamic value of the energy for $K = 3$ as a function of T in Fig. 9. The extrapolated values by the form including the next leading correction term are consistent with those by the paramagnetic solution at $T > 0.9$ and those by the 1RSB solution at

low temperatures, though a systematic deviation still remains around T_c because of the critical fluctuation. As shown in the inset of Fig. 9, the agreement between the extrapolated value and the value of 1RSB solution is held at very low temperatures and the limiting value of energy at zero temperature coincides with that obtained by zero-temperature calculations[14, 31, 32, 33]. For the case of $K = 3$, the result of the cavity method is also shown in Fig. 9[16]. Analytic results are in good agreement with the MC data at low temperatures. These support the validity of the scheme also for $K = 3$.

Before closing this section, we would like to mention MC algorithm for studying SG models. In recent works[16, 34], it is claimed that in annealing simulations a slow annealing limit of the energy often leads to the iso-complexity energy, significantly above the static equilibrium energy in glassy systems. This has been confirmed for $K = 3$ by an annealing simulation[16]. In contrast, as shown in Fig. 9, the energy extrapolated to the infinite-volume limit in our exchange MC results is well lower than the iso-complexity energy and is compatible with that of the 1RSB solution at low temperatures. This suggests that the exchange MC is suitable for equilibration of the SG system even when the system have the iso-complexity energy separated from the static one.

IV. SUMMARY AND DISCUSSION

We have studied a construction of a 1RSB solution for quench disordered systems. Our construction is based on thermodynamic conditions for the cumulant generating function $\phi(n)$ of free energy, which are derived as a necessary condition in the replica analysis. The only requirement for our construction is to obtain the replica symmetric solution for $\phi(n)$ as a function of n . This is a quite general scheme which may provide an unified way to give a correct solution for 1RSB systems. In fact, our scheme reproduces the well-known 1RSB solution for fully connected mean-field SG models such as p -spin model[10] and Potts glass model[35]. As a non-trivial example we have applied our scheme to study a 1RSB solution for finite-connectivity Ising SG models with K -spin interactions. The thermodynamic quantities are explicitly evaluated from numerically obtained RS solution with finite replica number n using our scheme.

The saddle-point equations to be solved in our scheme are found to be equivalent to recursion equations of the cavity-field distributions in the 1RSB cavity formalism for this model. In a sense, our scheme based on the replica theory can be regarded as a reinterpretation of the 1RSB cavity method. While the cavity method can predict the microscopic detail of a model through complexity, which is an interesting quantity in glassy physics, one cannot obtain such a quantity with our scheme at present. This would be discussed as a remaining issue. In contrast, we can construct the 1RSB theory irrespective of details of the model, even non-mean-field

model in principle, because our scheme does not rely on the microscopic details, or complexity. Since the pure state in finite dimensions is difficult to formulate in a tractable manner, this complexity-independent formalism of 1RSB may be useful to investigate nature of RSB in finite dimensions[36]. Because the replica method itself is originally independent of calculus of spin variables, this theoretical flexibility would give another perspective if RSB is formulated within macroscopic level. Therefore, we consider that the cavity method and our method are complementary in order to understand the nature of SG. The correspondence of their results in this model has a significance because they should provide the same result in the intersection of their validity range.

Unfortunately, the validity of our 1RSB solution could not be established within the scheme because of the lack of AT analysis. Some AT analyses for finite-connectivity models are recently proposed in the previous works[18, 31, 37]. They are to be resolved for our model and compared with each other in future study. To confirm the validity of our scheme in the present work, equilibrium MC simulations with the help of extended ensemble method have been performed for the model with $K = 2$ and 3. It is shown that for $K = 2$, the resulting thermodynamic quantities by our scheme are in agreement with those obtained by MC simulation within statistical error. For $K = 3$, assuming that the size dependence of the thermodynamic quantities is expressed as a polynomial of N^{-1} , we have concluded that our 1RSB solution is also consistent with those extracted from the finite-size MC data. If we have the correction exponent ω a priori, we can promote the accuracy of our extrapolation. Optimization techniques for ground-state search would be a promising approach for estimating the value of ω for $K = 3$.

As a by-product of the MC simulations, it is found that a coefficient of the first finite-size-correction term is positive. Namely, the finite-size data reach their thermodynamic value from above with increasing the system size. This suggests that fluctuations on the positive side of the thermodynamic value is relevant for the finite-size corrections in these models. On the other hand, the probability of large deviations which can be calculated using the replica theory with $n > 0$ is the negative side for the free energy in the fully connected SK model[38]. The replica theory with $n < 0$ for the large deviations is required to evaluate the finite-size correction.

The key ingredient in our scheme for constructing the 1RSB solution is the thermodynamic constraints as a necessary condition in the replica theory. This is compared to the fact that the standard replica method introduces RSB scheme through the symmetry of the saddle point. Another thermodynamic constraint, thermodynamic homogeneity, has been discussed in Ref. 39. One might stress the importance of such a thermodynamical approach which leads to an universal framework irrespective of microscopic models. Actually, our scheme is rather general and quite simple. It only needs the func-

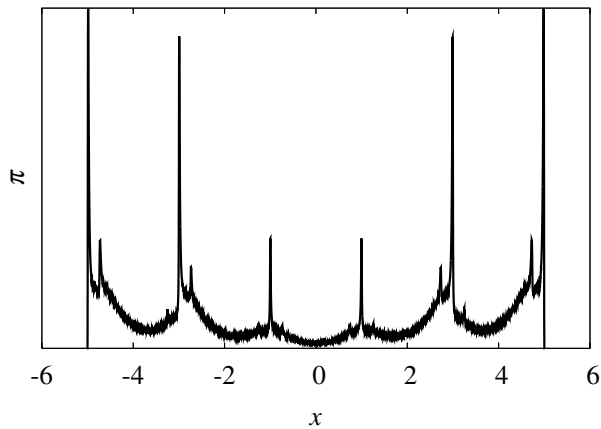


FIG. 10: A saddle-point function $\pi(x)$ for $K = 3, C = 6, T = 0.75$ and $n = 0.713$.

tion $\phi_{\text{RS}}(n)$ which is constructed in the way of replica symmetric analysis. Thus, we can avoid the arbitrariness to introduce breaking parameter in the replica theory. One can find further applications in related statistical-mechanical systems in which the RS solution can be constructed.

Acknowledgments

We would like to thank Y. Kabashima for helpful comments and discussions, and for explaining the details of algorithm for solving the saddle-point equations[40]. We are also grateful to F. Krzakala for making his numerical data in Ref. [18] available to us. TN also gratefully acknowledges K. Mimura for the kind and helpful lecture. He is strongly inspired by the lecture. This work was supported by the Grant-in-Aid for Scientific Research on the Priority Area “Deepening and Expansion of Statistical Mechanical Informatics” (No. 1807004) by Ministry of Education, Culture, Sports, Science and Technology, Japan.

APPENDIX A: ALGORITHM FOR EVALUATING π AND $\hat{\pi}$

In this appendix, we explain details of the numerical method we used to solve the saddle-point equations (9)

and (10). We use an iteration method, introduced in Ref. 40. The saddle-point functions $\pi(x)$ and $\hat{\pi}(\hat{x})$ are approximated by a large M number of samples from π and $\hat{\pi}$. The algorithm for evaluating the function $\pi(x)$ and $\hat{\pi}(\hat{x})$ is as follows:

1. Give an appropriate array $h_i (i = 1, 2, \dots, M)$ as an initial condition to π .
2. Sample $K - 1$ independent values of $\{x_k\} (k = 1, \dots, K - 1)$ from $\pi(x)$ by generating a random integer I uniformly distributed from 1 to M and setting $x_k = h_I$, and evaluate $\hat{x} = \frac{1}{\beta} \text{atanh} \left(\tanh \beta \prod_{k=1}^{K-1} \tanh(\beta x_k) \right)$.
3. Put the sign chosen with probability 1/2 to \hat{x} and get $\hat{h}_i = \hat{x}$, which corresponds to a sample of $\hat{\pi}$.
4. Repeat the steps 2 and 3 M times and obtain the M samples of $\hat{\pi}, \{\hat{h}_i\}$.
5. Sample $C - 1$ independent values of $\{\hat{x}_\gamma\} (\gamma = 1, \dots, C - 1)$ by a procedure similar to that of step 2 and evaluate $x = \sum_{\gamma=1}^{C-1} \hat{x}_\gamma$.
6. Accept x obtained in step 5 with probability $\frac{1}{2^{n(C-1)}} \left\{ \prod_{\gamma=1}^{C-1} (1 + \tanh(\beta \hat{x}_\gamma)) + \prod_{\gamma=1}^{C-1} (1 - \tanh(\beta \hat{x}_\gamma)) \right\}^n$ and accumulate a new set of $\{h_i\}$ of π till the number reaches M .
7. Return to 2.

We iterate the above procedures until convergence. The number of the samples is set typically as $M = 10^6$ in our calculation. A typical form of $\pi(x)$ is displayed in Fig. 10.

[1] S. F. Edwards and P. W. Anderson, *J. Phys. F* **5**, 965 (1975).
[2] G. Parisi, *J. Phys. A* **13**, L115 (1980).
[3] M. Mézard, G. Parisi, and M. Virasoro, *Spin Glass Theory and Beyond* (World Scientific Publishing, Singapore, 1987).

[4] M. Talagrand, *Ann. Math.* **163**, 221 (2006).
[5] S. Kirkpatrick and D. Sherrington, *Phys. Rev. B* **17**, 4384 (1978).
[6] J. R. L. de Almeida and D. J. Thouless, *J. Phys. A* **11**, 983 (1978).
[7] I. Kondor, *J. Phys. A* **16**, L127 (1983).

- [8] E. Gardner, Nucl. Phys. B **257**, 747 (1985).
- [9] D. J. Gross, I. Kanter, and H. Sompolinsky, Phys. Rev. Lett. **55**, 304 (1985).
- [10] T. Nakajima and K. Hukushima, J. Phys. Soc. Jpn. **77**, 074718 (2008).
- [11] P. Y. Lai and Y. Y. Goldschmidt, J. Phys. A **22**, 399 (1989).
- [12] Y. Y. Goldschmidt and C. D. Dominicis, Phys. Rev. B **41**, 2184 (1990).
- [13] M. Mézard and G. Parisi, Euro. Phys. J. B **20**, 217 (2001).
- [14] S. Franz, M. Leone, F. Ricci-Tersenghi, and R. Zecchina, Phys. Rev. Lett. **87**, 127209 (2001).
- [15] S. Franz, M. Mézard, F. Ricci-Tersenghi, M. Weigt, and R. Zecchina, Europhys. Lett. **55**, 465 (2001).
- [16] A. Montanari and F. Ricci-Tersenghi, Phys. Rev. B **70**, 134406 (2004).
- [17] M. L. S. Franz and F. Toninelli, J. Phys. A **36**, 10967 (2003).
- [18] F. Krzakala and L. Zdeborová, Europhys. Lett. **81**, 57005 (2008).
- [19] M. Mézard, F. Ricci-Tersenghi, and R. Zecchina, J. Stat. Phys. **111**, 505 (2003).
- [20] R. Monasson, Phys. Rev. Lett. **75**, 2847 (1995).
- [21] K. Ogure and Y. Kabashima, Prog. Theor. Phys. **111**, 661 (2004).
- [22] M. Wong and D. Sherrington, J. Phys. A **20**, L793 (1987).
- [23] K. Mimura, (private communication).
- [24] K. Mimura, J. Phys. A **2009**, 135002 (42).
- [25] D. J. Thouless, Phys. Rev. Lett. **56**, 1082 (1986).
- [26] G. Parisi, e-print arxiv:cond-mat/031157.
- [27] K. Hukushima and K. Nemoto, J. Phys. Soc. Jpn. **65**, 1604 (1996).
- [28] A. M. Ferrenberg and R. H. Swendsen, Phys. Rev. Lett. **63**, 1195 (1989).
- [29] T. Murayama and M. Okada, J. Phys. A **36**, 11123 (2003).
- [30] S. Boettcher, Euro. Phys. J. B **31**, 29 (2003).
- [31] A. Montanari and F. Ricci-Tersenghi, Euro. Phys. J. B **33**, 339 (2003).
- [32] M. Mézard and G. Parisi, J. Stat. Phys. **111**, 1 (2004).
- [33] P. Y. Lai and Y. Y. Goldschmidt, J. Phys. A **23**, 3329 (1990).
- [34] F. Krzakala, M. Tarzia, and L. Zdeborová, Phys. Rev. Lett. **101**, 165702 (2008).
- [35] T. Nakajima and K. Hukushima, (unpublished).
- [36] T. Temesvári, Nucl. Phys. B **772**, 340 (2007).
- [37] T. Obuchi, Y. Kabashima, and H. Nishimori, J. Phys. A **42**, 075004 (2009).
- [38] G. Parisi and T. Rizzo, Phys. Rev. Lett. **101**, 117205 (2008).
- [39] V. Janiš and L. Zdeborová, Prog. Theor. Phys. Suppl. **157**, 99 (2005).
- [40] Y. Kabashima, N. Sazuka, K. Nakamura, and D. Saad, Phys. Rev. E **64**, 046113 (2001).